# Proposal for a New Threshold Stress Intensity Factor Range Equation for Fatigue Crack Propagation and a Study on the Analysis of Peculiar Fracture Behavior of Shot Peened Materials by its Application

Ki-Woo Nam[1], Kotoji Ando[2], and Min-Heon Kim[1]

[1]Pukyong National University
[2]Yokohama National University

May 6, 2020

## Abstract

An equation of the threshold stress intensity factor range was proposed for the fatigue crack growth using a nonlinear region of unique fatigue fracture. The following phenomena, peculiar to the peening specimen with a pre-crack, were analyzed using previous experiment results based on the proposed equation. As a result, the following to phenomena could be evaluated quantitatively whereas was evaluated qualitatively. Pre-crack size that can be rendered harmless by peening; Fatigue limit of pre-crack specimen that cannot be rendered harmless; A phenomenon that fatigue fracture appears from outside the pre-cracked part on most of the harmless pre-crack specimen; Non-propagating crack condition of stage II (tensile type), observed in most specimen showing fatigue limit; and Qualitative analysis for initiation of non-propagating stage II crack (tensile type) in the peening specimen based on the reference regarding to a micro distribution of residual stress due to peening.

## 1 | INTRODUCTION

Hadadd et al.[1] proposed an equation with which to evaluate the fatigue limit of micro crack materials, and showed that the equation can be used to accurately evaluate the fatigue limits of micro crack materials. There are two characteristics of this equation: A crack length $2l$ in an infinite plate is assumed to be$2(l+l_o)$, the threshold stress intensity factor range $(K_{th(l)})$ for fatigue crack propagation is assumed to be a constant value, as shown in the following Equation 1.

$$K_{\text{th}} = \sigma_w \sqrt{\pi(l + l_o)} \ (1)$$

Where $\sigma_w$ is the fatigue limit of a smooth specimen.

Kitagawa et al.[2] experimentally demonstrated that the threshold stress intensity factor range $(K_{\text{th}})$ of fatigue crack propagation of micro crack becomes smaller as the crack length is shortened. $K_{\text{th}}$ is divided into the threshold stress intensity factor $(K_{th(s)})$ for shot cracks that depend on the crack length and the threshold stress intensity factor $(K_{th(l)})$ for long cracks that do not depend on the crack length. Tange et al.[3] defined the threshold stress intensity factor range $(K_{th(s)})$ of short cracks for the intermediate crack length $(l)$ of crack length $(l_0)$ and $(l + l_0)$ of the infinite plate; this is shown in Equation 2.

$$K_{th(s)} = \sigma_{\text{wc}} \sqrt{\pi\lambda} \quad (2)$$

Where $\sigma_{\text{wc}}$ is the fatigue limit of the crack specimen. Tange et al.[3] obtained Equation 3 by removing$l_0$ from Haddad's[1] equation. This equation can be used to evaluate the dependence of the crack dimension of$K_{th(s)}^R$

1

when a semi-elliptical surface crack exists in a finite plate of stress ratio R.

$$\Delta K_{\text{th}}^{R} = \left\{ \left( \frac{1}{\Delta K_{th(l)}^{R}} \right)^{2} + \left( \frac{1}{\gamma \Delta \sigma_{w}^{R} \sqrt{\pi \alpha}} \right)^{2} \right\}^{-0.5} \qquad \textbf{(3)}$$

Where $K_{\text{th}}^{R}$ is the stress intensity factor of a certain crack, $K_{th(l)}^{R}$ is the threshold stress intensity factor of a long crack, $\sigma_{w}^{R}$ is the fatigue limit of a smooth specimen, superscript R is the stress ratio, and $\gamma$ is the crack shape correction factor of a finite plate, according to the Newman-Raju equation.[4]

$K_{th(l)}$ of long cracks is constant, but $K_{th(s)}$ of short cracks decreases as the cracks become shorter. These phenomena have been found in brittle fracture and hydrogen embrittlement[5]of metals[6] and ceramics.[7,8] This is because a long crack satisfies small-scale yielding conditions (small-scale nonlinear region conditions, in the case of ceramics), but a short crack does not satisfy these conditions. Therefore, it is necessary to suggest an equation of $K_{th(s)}$ of micro fatigue crack under the assumption that the small-scale yielding conditions are not satisfied. A fatigue fracture evaluation diagram considering the compression yield zone size at unloading and cyclic yield stress has been proposed.[9,10] However, this method requires evaluating the cyclic yield stress and the equation becomes complicated.

In this paper, a new $K_{th(s)}$ evaluation equation is proposed that focuses on nonlinear behavior at the fatigue limit substantially lower than the yield stress. Further, the peculiar fatigue fracture behavior of peened material was analyzed using this equation. The results were quantitatively explained and reported for all items except for the initiation conditions of the stage II (tensile type) non-propagating crack which were mentioned in Chapter 3. The initiation conditions of the non-propagating crack in stage II were easily explained by focusing on the micro residual stress distribution of the peened material.

## 2 | PROPOSAL OF EQUATION FOR THRESHOLD STRESS INTENSITY FACTOR RANGE OF FATIGUE CRACK PROPAGATION

It is assumed that an infinite plate with a through crack of a length ($2l$ ) is subjected to a cyclic tensile stress ($\sigma^{R}$) with a stress ratio (R[?]0). The fatigue limit ($\Delta \sigma_{w}^{R}$) of a smooth specimen shows nonlinear behavior as follows. Although the maximum tensile stress ($\Delta \sigma_{\text{wm}}^{R}$) at the fatigue limit of a smooth specimen is lower than the yield stress $\sigma_{y}$, slip bands are formed at many grains as a result of the cyclic effect. These slip bands become active, thus forming intrusions and extrusions.[11] Based on this, the maximum stress ($\Delta \sigma_{\text{wm}}^{R}$) of the fatigue limit of the smooth specimen given in Equation 4 can be considered the standard stress of the nonlinear area evaluation of the crack material showing the fatigue limit.

$$\sigma_{\text{wm}}^{R} = \frac{\Delta \sigma_{w}^{R}}{(1-R)} \qquad (4)$$

The maximum stress ($\Delta \sigma_{\text{wcm}}^{R}$) at the fatigue limit ($\Delta \sigma_{\text{wc}}^{R}$) of the crack material are given by the following Equation 5.

$$\sigma_{\text{wcm}}^{R} = \frac{\Delta \sigma_{\text{wc}}^{R}}{(1-R)} \qquad (5)$$

As is the case in situations such as brittle fracture[5-8] of metal material or ceramics, the dimensions of the nonlinear region formed on the crack tip and the growth conditions of the fatigue crack are set under the following three assumptions. The dimension ($P_{\text{NF}}^{R}$) of the nonlinear region formed at the fatigue crack tip is given by Dugdale's equation[12] using $\sigma_{\text{wm}}^{R}$ and$\sigma_{\text{wcm}}^{R}$. When the nonlinear region formed at the fatigue crack tip is above a certain limit value ($P_{\text{NFC}}^{R}$), the fatigue crack propagates, but it does not propagate below the

limit value. The limit value $(P_{\mathrm{NFC}}^R)$ does not depend on the crack length. Thus, $P_{\mathrm{NFC}}^R$ is given by Equation 6.

$$P_{\mathrm{NFC}}^R = l \left\{ \sec \left( \frac{\pi \sigma_{\mathrm{wcm}}^R}{2 \sigma_{\mathrm{wm}}^R} \right) - 1 \right\} \qquad (6)$$

The limit value $(P_{\mathrm{NFC}}^R)$ of the nonlinear region in Equation 6 does not depend on the crack length. Since $\left( \frac{\pi \sigma_{\mathrm{wcm}}^R}{2 \sigma_{\mathrm{wm}}^R} \right)$ is very small when the crack is very long, the sec term can be approximated sufficiently in the series expansion up to the second term. The threshold stress intensity factor range $(K_{th(l)}^R)$ of a long crack is given by Equation 7.

$K_{th(l)}^R = \sigma_{\mathrm{wc}}^R \sqrt{\pi \lambda}$ (7)

Therefore, Equation 6 can be expressed by Equation 8.

$$P_{\mathrm{NFC}}^R = l \left\{ \sec \left( \frac{\pi \Delta \sigma_{\mathrm{wc}}^R}{2 \Delta \sigma_w^R} \right) - 1 \right\} = \frac{\pi}{8} \left( \frac{\Delta K_{th(l)}^R}{\Delta \sigma_w^R} \right)^2 \qquad (8)$$

Since the right side of Equation 8 is a constant, the relationship between the crack length $(l)$ and $\sigma_{\mathrm{wc}}^R$ can be obtained from the second term. When there is a through crack of length $2l$ in an infinite plate, the threshold stress intensity factor range $(K_{th(s)}^R)$ of a short crack can be evaluated using Equation 9.

$K_{th(s)}^R = \sigma_{\mathrm{wc}}^R \sqrt{\pi \lambda}$ (9)

Substituting Equation 9 into Equation 8 becomes Equation 10, an equation for evaluating the crack length dependence of the threshold stress intensity factor range.

$$\Delta K_{th}^R = 2 \Delta \sigma_w^R \sqrt{\frac{c}{\pi}} \left[ \left\{ \frac{\pi}{8c} \left( \frac{\Delta K_{th(l)}^R}{\Delta \sigma_w^R} \right)^2 + 1 \right\}^{-1} \right] \qquad (10)$$

Equation 10 considers infinite plates. When applying Equation 10 to a finite plate with a semi-elliptical crack, substitute the equivalent crack length $(le)$ in Equations 11 and 12 for the crack length $(l)$ in Equation 10.

$$\sqrt{\pi l_e} = \alpha_A \sqrt{\pi \alpha} \qquad (11)$$

$$\sqrt{\pi l_e} = \beta_A \sqrt{\pi \alpha} \qquad (12)$$

Where $a$ is the semi-elliptical crack depth and $\alpha_A$ and $\beta_A$ are the shape correction factors given by the Newman–Raju equation[4] at the deepest crack part (point A) when the specimen of the finite plate is subjected to tensile or bending stress, respectively. When evaluating $l_e$ corresponding to the outermost surface part (point C), $\alpha_A$ and $\beta_A$ are substituted to $\alpha_C$ and $\beta_C$, respectively, corresponding to the shape correction factors at point C.

The fatigue limit of high strength nitride steel[13] and spring steel[14] was analyzed in the case where a finite plate with a micro semi-elliptical crack was subjected to bending stress. The analytical and experimental values obtained by Equations 10-12 showed good agreement regardless of the crack size, crack aspect ratio and stress ratio (R).

## 3 | EXPERIMENTAL RESULTS USED FOR ANALYSIS

Recently, many papers examining the fatigue fracture behavior of peened crack materials have been published.[15-20] Typical examples of the experimental results are shown in Figures 1-3.[15] The material is spring steel of HV470, and the width ($2W$) and thickness ($t$) of the specimen are 10mm and 3mm, respectively. The arithmetic average roughness (Ra) of the specimen surface is 4.76$\mu$m. Figure 1 shows the residual stress distribution due to shot peening.
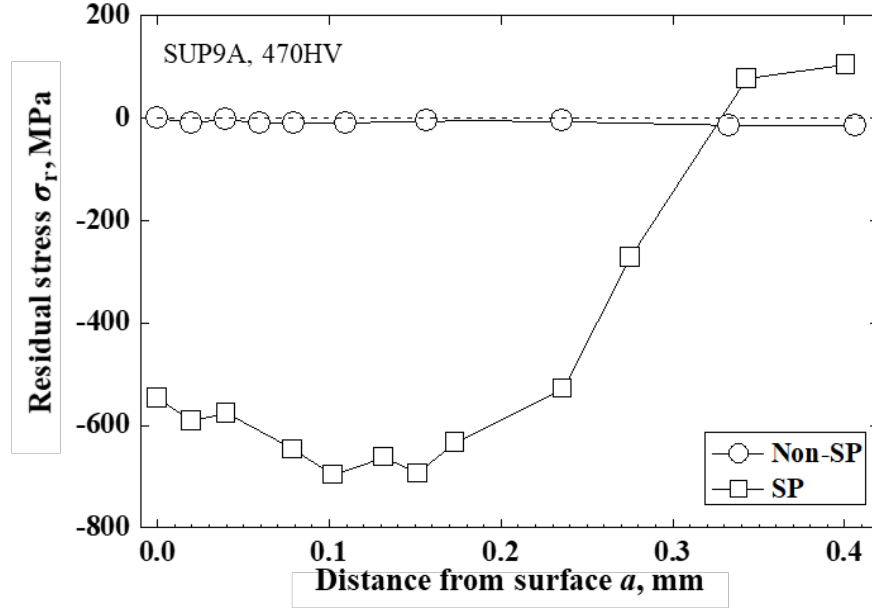


**FIGURE 1** Residual stress distribution by shot peening[15]

A semi-elliptical slit with a width of 0.05mm was machined on the surface of a specimen by electric discharge machining. The aspect ratio of the slit ($As =a /c$) was 1.0 and 0.4, where $a$ is the depth of the semi-elliptical crack and $2c$ is the crack length on the surface. The depths of the slits for each $As$ are of three types, either 0.1, 0.2, or 0.3 mm. Each slit is as sharp as a crack. Hereinafter, the slit specimen will be referred to as a pre-crack specimen. The fatigue tests were carried out in the bending test of stress ratio (R=0).

Figure 2 shows the fatigue limits of the non-peening specimen (hereinafter, the Non-SP specimen) and the peening specimen (hereinafter, the SP specimen). Figure 2(a) and (b) show the results of $As =1.0$ and 0.4, respectively. The fatigue limit was obtained from only three specimens of the Non-SP specimen, and the average fatigue limit was 860 MPa. For the SP specimen, eight out of 16 specimens whose pre-cracks were rendered harmless showed the fatigue limit. The highest fatigue limit was 960MPa and the lowest was 880MPa. The average fatigue limit of the SP specimen was determined to be 900MPa. The rendered harmless pre-crack was defined as the fatigue limit of the SP pre-crack specimen was not less than 95% of the fatigue limit of the SP smooth specimen.[15-20] The threshold stress intensity factor range ($K_{\text{th}(l)}$) for the long crack was 6.09MPa$\sqrt{m}$.[15]

1. As=1.0
2. As=0.4

**FIGURE 2** Relationship between fatigue limit and crack depth for Non-SP and SP specimens of SUP9A [aspect ratio $a /c =1.0$ and 0.4][15]

The SP specimen showing the fatigue limit was heated at 280ºC for one hour after the test and fractured under high cyclic stress. As shown in Figure 3, most of the specimens showed tensile type stage II non-propagating cracks.[15]

4

The results[15-20] of many previous experimental studies have highlighted four problems with the peculiar fatigue fracture behavior of SP pre-crack specimens. Regarding Figures 2 and 3, the following should be clarified in terms of the four problems and Equations 10-12:

1. The pre-crack specimens of $a$ =0.1 and 0.2mm, which can reduce about 50 70% of the fatigue limits of Non-SP specimens, could be rendered harmless. Can the maximum depth ($a_{\mathrm{hlm}}$) of harmless pre-cracks be accurately evaluated?
2. Can the fatigue limit of an SP specimen of $a$ =0.3 mm that cannot be rendered harmless be accurately evaluated?
3. When the pre-crack specimens of $a$ =0.1 and 0.2mm in the SP specimen were fatigue fractured at stresses exceeding the fatigue limit, most of the specimens (those with * marks) fractured outside the pre-crack part. Can this phenomenon be explained?
4. When the SP smooth specimen and the SP pre-crack specimen ($a$ =0.1 and 0.2 mm) showed the fatigue limit, a stage II (tensile type) non-propagating crack was observed in most of the specimens, as shown in Figure 3. Can the crack initiation and the presence of non-propagating cracks be explained?
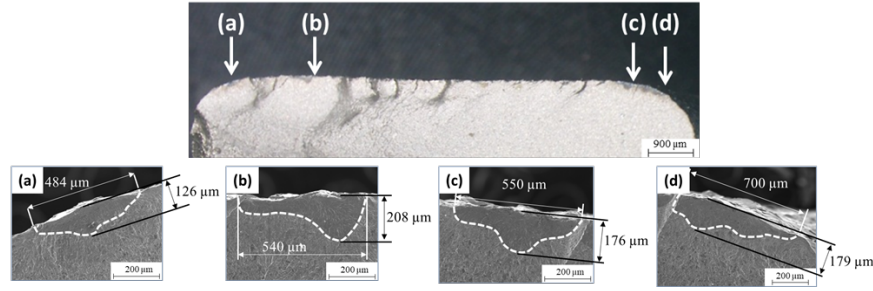


**FIGURE 3**    Stage II non-propagating crack in SP specimen [Fatigue limit = 920MPa][15]

## 4 | ANALYSIS METHOD AND RESULTS

### 4.1 | Analysis method

The stress intensity factor range ($K_{\mathrm{ap}}$) caused by applied stress was evaluated using the Newman-Raju equation,[4] and the stress intensity factor ($K_r$) by compressive residual stress was evaluated using the API equation.[21]

Since the analyzed experiment was carried out at R=0, the effective stress intensity factor range ($K_{\mathrm{Tr}}$) was evaluated using Equation 13.

$$K_{\mathrm{Tr}} = K_{\mathrm{ap}} + K_r \quad (13)$$

The harmless maximum crack depth ($a_{\mathrm{hlm}}$) is given by Equation 14.

$K_{\mathrm{Tr}} = K_{th(s)} \ (14)$

The effective value ($K_{\mathrm{TrA}}$) at point $A$ of [?]K that reduces the fatigue limit ($\sigma_{\mathrm{wsp}}$) of the SP smooth specimen is given by Equation 15.

$K_{\mathrm{Tr}RA} = K_{\mathrm{TrA}} - K_{th(s)A} \qquad (15)$

In addition, point $C$ is obtained by substituting $A$ with $C$ in Equation 15.

The reduction value of the fatigue limit at point $A (\sigma_{\mathrm{wcR}})$ is given by Equation 16.

$K_{\mathrm{Tr}RA} = \beta_A \sigma_{\mathrm{wcR}} \sqrt{\pi \alpha} \quad (16)$

Where $\beta_A$ is the shape correction factors given by the Newman–Raju equation[4] at the deepest crack point when the specimen of the finite plate is subjected to bending stress. Point $C$ is also calculated using the same method, and the smaller fatigue limit is used from points A and B.

### 4.2 | Evaluation of maximum harmless crack depth ($a_{hlm}$) of SP specimen

Figure 4 shows the relationship between $K_{th(s)}$ and crack depth ($a$) for the deepest part (point $A$) and the crack surface (point $C$) of the SP specimen. (a) and (b) are the results of $As$ =1.0 and 0.4, respectively. The stress intensity factor range ($K_{Tr}$) of the residual stress region was evaluated using Equation 13 and is shown in Figure 4. $K_{th(s)}$ and $K_{Tr}$ were evaluated at points A and C, and were respectively shown as $K_{th(s)A}$ and $K_{th(s)C}$, and as $K_{TrA}$ and $K_{TrC}$. In the figure, the short crack depth ($a$) at the intersection of $K_{th(s)A}$ and $K_{TrA}$, $K_{th(s)C}$ and $K_{TrC}$ is the maximum crack depth ($a_{hlm}$) that can be rendered harmless. In Figure 4(a) and (b), $As$ =1.0 and 0.4 are $a_{hlm}$=0.271mm and 0.242mm, respectively. Based on the experimental results in Figure 2(a) and (b), the crack sizes of $a$ =0.1mm and 0.2mm were rendered harmless, but $a$ =0.3mm was not rendered harmless. Therefore, it can be said that the results of experimentation and calculation were qualitatively matched.
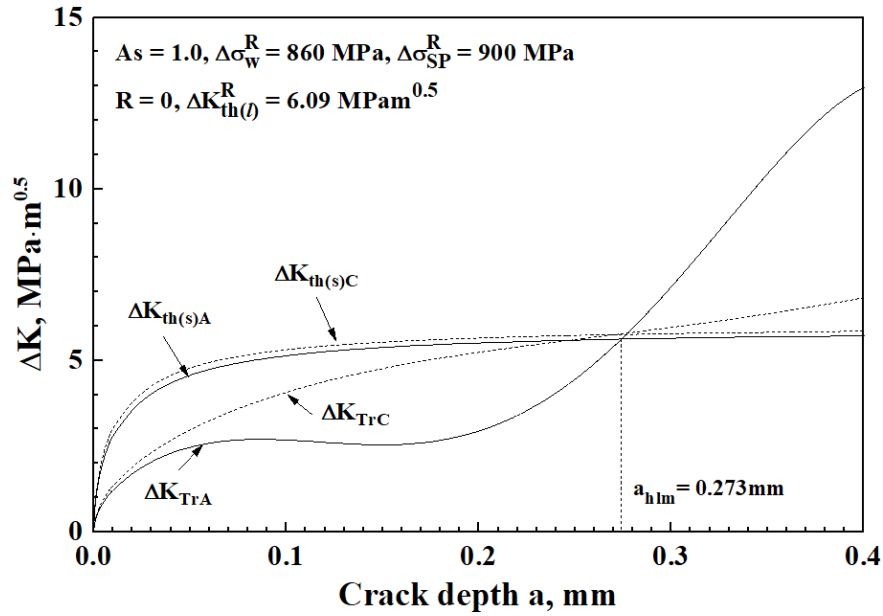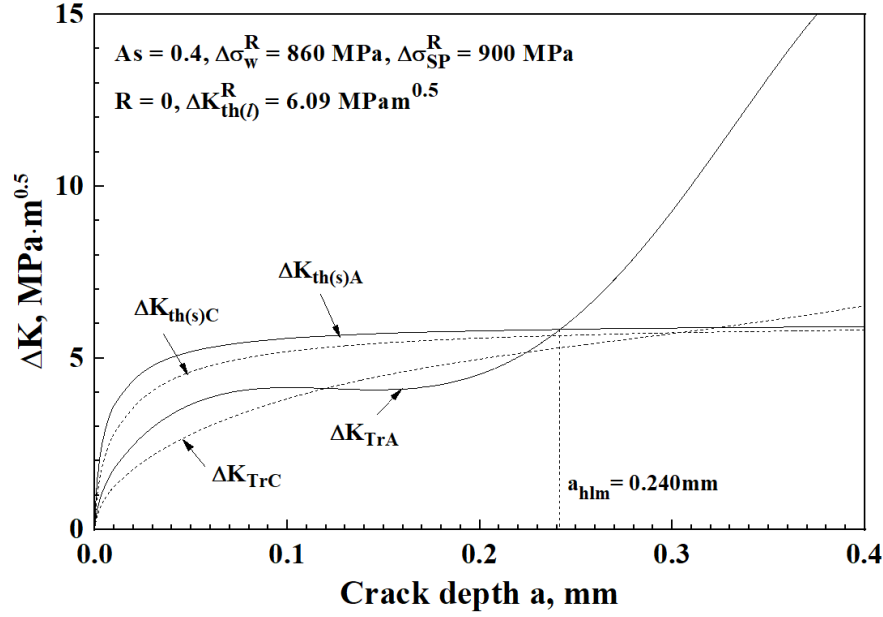
**FIGURE 4**   Crack depth dependence of $K_{th(s)}$ and $K_{Tr}$ of $A$ and $C$ points

### 4.3 | Evaluation of fatigue limit of SP crack specimen which cannot be rendered harmless

Table 1 shows the evaluation results of the fatigue limit of the SP crack specimen ($a$ =0.3mm) that cannot be rendered harmless using Equations 15 and 16. When the fatigue limit of the SP smooth specimen is considered to be considerably distributed to 880MPa~960MPa, the calculation and experimental results presented in Table 1 can be considered valid. The above and 4.2 clause results indicate that the harmless maximum crack depth ($a_{hlm}$ ) evaluated by Equations 10-12 proposed in this paper is quantitatively consistent with the experimental results.

**TABLE 1**   Evaluation results of fatigue limit

| a (mm) | Aspect Ratio As | experimental $\Delta\sigma_{wcSP}$ (MPa) | calculate $\Delta\sigma_{wcSP}$ (MPa) |
|--------|-----------------|------------------------------------------|----------------------------------------|
| 0.3 | 1.0 | 720 | 812 |
| 0.3 | 0.4 | 720 | 765 |

### 4.4 | Discussion of the SP pre-crack specimen having fracture behaviors from outside the pre-crack part under high stress exceeding the fatigue limit

If an SP pre-crack specimen with a harmless surface crack undergoes the fatigue test at high stress above the fatigue limit, it is often fractured outside the pre-crack part, despite the existence of a pre-crack that reduces more than 50% of the fatigue limit of the Non-SP specimen. Table 2 shows the results of fatigue testing. In Table 2, what was fractured outside the pre-crack part is labeled 'Out PC', while what was fractured in the pre-crack part is labeled 'From PC'. These results were obtained using Equations 10-12. The results are calculated as Figure 4 for various $As$ of specimens that fractured under stress exceeding the average fatigue limit of the SP specimen. In addition, the case of "Instrusion + stage I (shear type crack) depth ($a_{gr}$)", in which stage II (tensile crack) crack propagation is possible due to tensile stress, was also discussed. The condition is given by Equation 14.

According to the results of various calculations, $As$ , which obtains the minimum crack depth $a_{gr}$ that satisfies the above equation, was as small as about 0.2 or less; it was also found that it was sufficient to consider
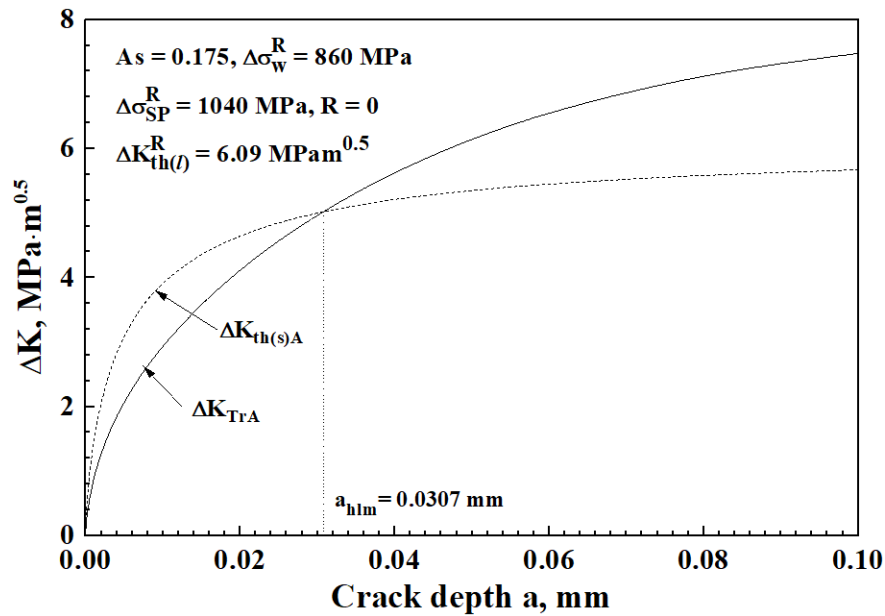
7

only the deepest crack part (point $A$ ). That is, $a_{\mathrm{gr}}$ was evaluated with various $As$, as shown in Figure 4, for a specimen that fractured under high stress exceeding the average fatigue limit (900MPa) of the SP specimen. Figure 5(a) and (b) show an example of the relationship between the minimum crack depth $a_{\mathrm{gr}}$, fatigue fracture stress, and $As$ . Table 2 shows all of the analysis results. With a fatigue fracture stress of 960MPa or higher, the specimen was fractured by the growth of Stage II (tensile type) cracks other than the pre-crack when $As$ was about 0.18 and $a_{\mathrm{gr}}$ was about 63 $\mu$m or more. However, when the fracture stress was lower than that, $a_{\mathrm{gr}}$ was large and the fracture behavior could not explained. This may be attributed to the following three reasons.

(a) The fatigue limit of the Non-SP smooth specimen is 840~880MPa and there is considerable dispersion. Therefore, the relationship between $K_{th(s)}$ and $a$ must also have a certain range.

(b) The fatigue limit of the SP specimen is 840~960MPa and there is considerable dispersion. The calculation has used the average value of 900MPa.

(c) As shown in the next section, when the residual stress of the SP specimen is measured microscopically, locally tensile residual stress can be found. Therefore, in the tensile residual stress part, stage II cracks occur much more easily than indicated by the calculation results in Table 2. This point will be discussed in detail in the next section. Based on these results, it can be concluded that the peculiar behavior of this section can be explained by the proposed Equations 10-12.
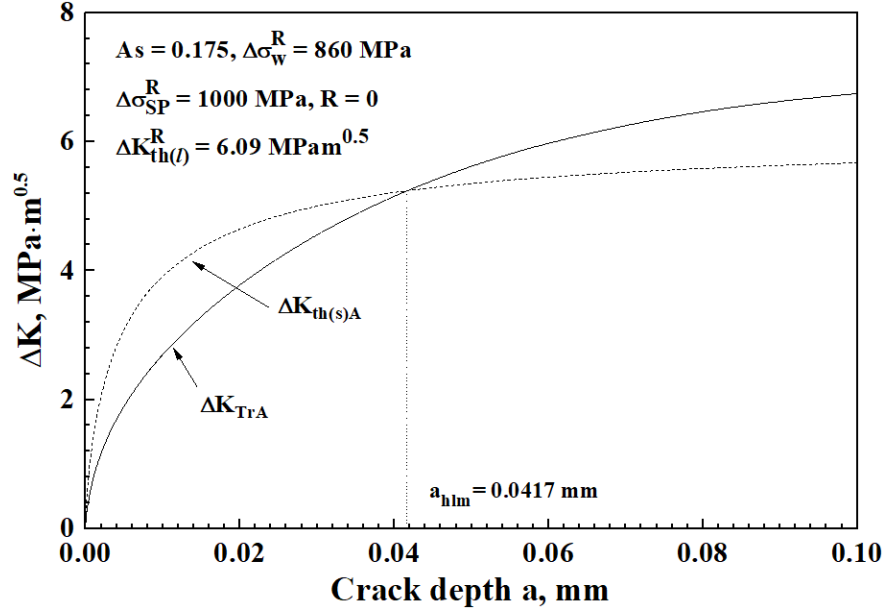
**TABLE 2** Evaluation results of $a_{\mathrm{gr}}$

| Stress range (MPa) | Experiment | Experiment | Calculation | Calculation |
|---|---|---|---|---|
| | $As=1.0$ | $As=0.4$ | $a_{\mathrm{gr}}$ ($\mu$m) | $As$ |
| 1040 MPa | Out PC | - | 30.7 | 0.175 |
| 1000 MPa | Out PC | Out PC | 41.7 | 0.175 |
| 960 MPa | Out PC | From PC | 62.7 | 0.180 |
| 920 MPa | Out PC | From PC | 201.9 | 0.205 |

Out PC: Fracture initiated from outside of pre-crack. From PC: Fracture initiated from pre-crack.



$As = 0.175$, $\Delta\sigma_W^R = 860$ MPa

$\Delta\sigma_{SP}^R = 1040$ MPa, R = 0

$\Delta K_{th(l)}^R = 6.09$ MPam$^{0.5}$

$\Delta K_{th(s)A}$

$\Delta K_{TrA}$

$a_{hlm} = 0.0307$ mm

(a)



(b)

**FIGURE 5** Evaluation of crack growth condition of SP specimen from outside of pre-crack (a)  Estimation of $a_{gr}$ ($\sigma_{SP}^R = 1040\ MPa$), and (b)  Estimation of $a_{gr}$ ($\sigma_{SP}^R = 1000\ MPa$)

## 5 | CONSIDERATION OF WHY STAGE II NON-PROPAGATING CRACKS INITIATE AND ARREST ON SP SPECIMEN

In the SP specimen showing the fatigue limit, a stage II (tensile type) non-propagating crack is observed in most of the specimens, as shown in Figure 3. Prior studies have attempted to analyze the initiation of stage II non-propagating cracks in SP specimens through macroscopic residual stress distribution and fracture mechanics. Takahashi[9] explained the case of R[?]0.05, but most previous studies[15-20] investigating the case of R[?]0 did not.

Investigations of the residual stress distribution of SP specimens in the literature have revealed that the residual stress distributions differ substantially between micro and macro measurements.[22] The measurement results of residual stress can be outlined as follows.[22] The measurement area was 0.8x0.8mm and the area was measured at a total of 81 points at 0.1mm intervals with a collimator diameter $\varphi = 10\~800\mu m$. In the case of 60% coverage at a collimator diameter of $\varphi=100\mu m$, the maximum tensile residual stress was 50MPa and the maximum compressive residual stress was -1100MPa. At a coverage of 300%, the maximum tensile residual stress was 200MPa and the maximum compressive residual stress was -1200MPa. In addition, the tensile residual stress was generated regardless of whether the part was convex(凸) or concave(凹). However, the average value of the residual stress measured in the 0.8x0.8 mm area was -630MPa regardless of the measurement direction.

The peening condition[15] that were analyzed in this paper were compared with those in Ref. (22). Peening was carried out by the same company in both cases, and all of the conditions were very similar. Table 3 compares the peening conditions used in the analysis of this paper and the peening conditions used in Ref. (22).

Based on the above, we assume that the micro maximum residual stress on the SP specimen surface, which was the sample of the analysis, is zero, and examine the crack initiation and non-propagating conditions for

Stage II based on that assumption. The fatigue limits of the Non-SP specimen and the SP specimen were 860MPa and 900MPa, respectively. If the local residual stress in the SP specimen was zero, stage II (tensile type) cracks would easily initiate in that part. However, if the stage II crack grows to some extent and its behavior becomes controlled by macro residual stress, then if the condition of $K_{\mathrm{Tr}}[?]K_{th(s)}$ is satisfied, the stage II crack will be arrested.

The stage II non-propagating crack shown in Figure 3 was observed at the $10^7$ cycle of a cyclic stress of 920MPa, which is about 2% higher than the average fatigue limit of the SP specimen of 900MPa. As shown in Figure 2, the crack shape was approximated to a semi-elliptical crack. Its $K_{th(s)}$, $K_{\mathrm{ap}}$, and $K_{\mathrm{Tr}}$ were evaluated, and the non-propagating crack condition was discussed. Although the crack shape was complicated, the measured values of the maximum crack depth and surface crack length were used. The results are shown in Figure 6. The $As$ of the four non-propagating cracks in Figure 3 differed from each other, but showed the $K_{th(s)}$ of average $As$ . $K$ in Figure 6 is the value corresponding to $K_{\mathrm{TrA}}$ ($\Delta$ symbol) and $K_{\mathrm{TrC}}$ (O symbol) at the deepest part of each of the non-propagating cracks shown in Figure 3. $K_{\mathrm{TrC}}$ and $K_{th(s)}$ are almost similar on the non-propagating cracks (b), (c), and (d), but for no-propagating crack (a), $K_{\mathrm{TrA}}$ and $K_{\mathrm{TrC}}$ are less than $K_{th(s)}$. However, considering that the maximum value on the crack depth was used when evaluating $K_{\mathrm{ap}}$, the $K_{\mathrm{TrC}}$ of the non-propagating cracks (b), (c), and (d) were evaluated to be slightly high. In view of the above, it is concluded that the four non-propagating crack phenomena of stage II can be explained quantitatively.

As described in section 4.4, if $As$ =0.2 or less, the non-propagating crack shows $K_{\mathrm{TrA}} > K_{\mathrm{TrC}}$, and the fatigue limit is determined by $K_{\mathrm{TrA}}$. For the non-propagating crack of about $As$ =0.6, it is actually observed that $K_{\mathrm{TrA}} < K_{\mathrm{TrC}}$, as shown in Figure 6, and the fatigue limit is determined by $K_{\mathrm{TrC}}$.

**TABLE 3** Condition of shot peening

|                            | This research | Past research |
| -------------------------- | ------------- | ------------- |
| Specimen                   | SUP9A         | SUP9A         |
| Specimen hardness          | 470HV         | 515HV         |
| Shot hardness              | 600HV         | 600HV         |
| Shot diameter              | 0.67mm        | 0.87mm        |
| Air pressure or shot speed | 0.63MPa       | 78m/s         |
| Coverage                   | 300%          | 60%, 300%     |

10
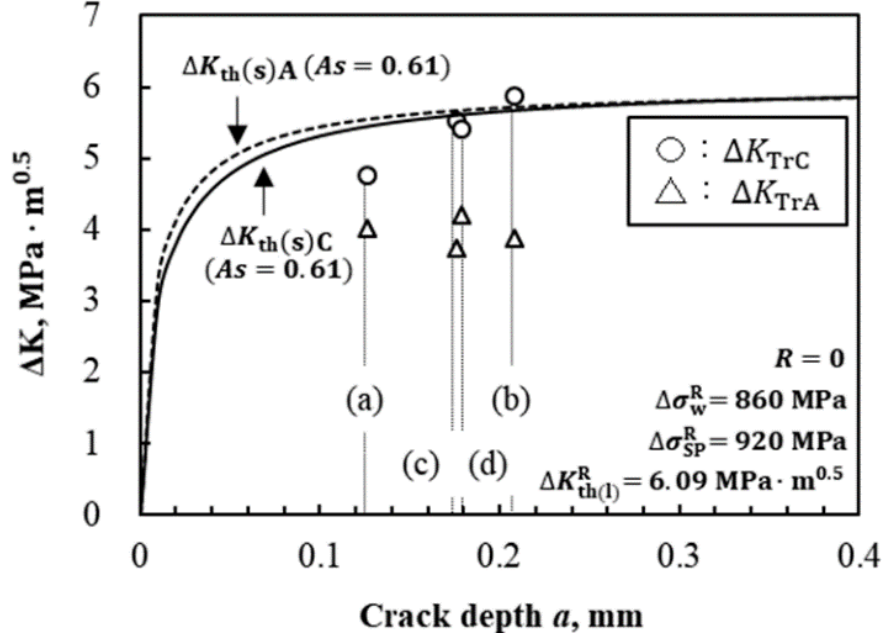
**FIGURE 6** $K_{\mathrm{TrA}}$ and $K_{\mathrm{TrC}}$ of non-propagating cracks

## 6 | CONCLUSIONS

In this study, a nonlinear region peculiar to fatigue fracture was defined and a new threshold stress intensity factor equation for fatigue crack growth was proposed. According to these, the fatigue fracture behavior of the shot peening specimen (SP specimen) was analyzed based on the experimental results for spring steel found in a previous study. The obtained results are as follows.

1) A nonlinear region peculiar to fatigue fracture was defined and a new threshold stress intensity factor equation for fatigue crack growth was proposed.

2) The maximum crack depth ($a_{\mathrm{hlm}}$) that can render a pre-crack harmless for an SP specimen was evaluated using Equations 10-12. The crack depth ($a$) that can be rendered harmless was experimentally found to be 0.1mm and 0.2mm, and the crack depth ($a$) that could not be rendered harmless was found to be 0.3mm. The crack depth value that can be rendered harmless was calculated to be between 0.2mm and 0.3mm.

3) The fatigue limits obtained through experimentation and calculation for the crack depth ($a$) of 0.3 mm, which cannot be rendered harmless for an SP specimen, were in relatively good agreement.

4) Based on the results of 2) and 3), the maximum crack depth ($a_{\mathrm{hlm}}$) that can be rendered harmless by the evaluated peening condition is judged to be a reasonable value.

5) For SP crack specimens with a crack depth of 0.2mm or less that could be rendered harmless, many specimens were fractured from outside the pre-crack, when stress exceeding the fatigue limit was applied. A crack depth of 0.2mm reduces more than 50% of the fatigue limit for Non-SP specimens. This behavior was explained by Equations 10-12, macro and micro residual stress distributions.

6) In most of the SP specimens showing the fatigue limit, a stage II non-propagating crack was observed. Although the crack initiation could not be explained by the macro residual stress distribution, it was qualitatively explained by considering the measurement results of the micro residual stress distribution.

7) Using the macro residual stress distribution and Equations 10-12, the non-propagating condition was investigated for many cracks. The non-propagating crack phenomena could be explained quantitatively.

11

**ORCID**

*Kotoji Ando*

*Min-Heon Kimhttps://orcid.org/0000-0001-8255-6341*

*Ki-Woo Namhttp://orcid.org/0000-0001-7019-358x*

**REFERENCES**

1. EI Haddad MH, Topper TH, Smith KN. Prediction of Non Propagating Cracks. *Eng Fract Mech* . 1979; 11: 573-584.

2. Kitagawa H, Takahashi S. Applicability of Very Small Cracks or Cracks in Early Stage. Proceedings of the second international conference on mechanical Behavior of materials. *ASM Int, Metals Park* , OH. 1976; 627-631.

3. Tange A, Akutu T, Takamura N. Relation between shot-peening residual stress distribution and fatigue crack propagation life in spring steel. *Transactions of JSSE* . 1991; 1991: 47-53.

4. Newman Jr JC, Raju IS. An Empirical Stress-Intensity Factor Equation for the Surface Crack. *Eng Fract Mech* . 1981; 15: 185-192.

5. Ando K, Fueki R, Nam KW, Matsui K, Takahashi K. A Study on the Unification of the Threshold Stress Intensity Factor for Micro Crack Growth. *Transactions of JSSE* . 2019; 64: 39-44.

6. Milne I, Ainsworth RA, Dowling AR, Stewart At. Assessment of the Integrity of Structures Containing Defects. CEGB Report R/H/R6-Rev. 1986; 3.

7. De Los Rios ER, Ando K, Biddulph RH. Fracture and Defect Assessment of Ceramic Composite. *Fatigue Fract Engng Mater Struct* . 1990; 13: 431-442.

8. Ando K, Kim BA, Iwasa M, Ogura N. Process zone size failure criterion and probabilistic fracture assessment curve for ceramics. *Fatigue Fract Engng Mater Struct* . 1992; 15: 139-149.

9. Takahashi F. Improvement of fatigue limit and acceptable surface defect size for spring steel by shot peening. Phd Treatise to Yokohama National University, (2008).

10. Takahashi F, Ando K, Takahashi K, Okada H, Oohashi M, Ebashi H. Development of fatigue limit analysis diagram. *J High Pres Inst Jpn* . 2008; 46: 344-351.

11. Forsyth PJE. Fatigue Damage and Crack Growth in Aluminum Alloys.*Acta. Metallurgica* . 1963; 11: 703-715.

12. Dugdale DS. Yielding of Steel Sheets Containing Slits. *J Mech Phys Solids* . 1960; 8: 100-104.

13. Konya J, Yamada Y, Takahashi K. Quantitative Evaluation of Influence of Surface Defects on Fatigue Limit of Nitrided Steel. *Transactions of JSSE* . 2019; 64: 45-51.

14. Ishii T, Takahashi K, Okada H. Effects of Small Surface Defect on Fatigue Limit of Spring Steel. *Transactions of JSSE* , (2020), (In Printing).

15. Nakagawa M, Takahashi K, Osada T, Okada H, Koike H. Improvement in Fatigue Limit By Shot Peening for High-strength Steel Containing Crack-like Surface Defect (Influence of Surface Crack Aspect Ratio).*Transactions of JSSE* . 2014; 59: 13-18.

16. Takahashi K, Amano T, Ando K, Takahashi F. Improvement of fatigue limit by shot peening for high-strength steel containing a crack-like surface defect. *Int J Struct Integrity* . 2011; 2: 281-292.

17. Takahashi K, Okada H, Ando K. Effects of shot peening on the torsional fatigue limit of high-strength steel containing an artificial surface defect. *Int J Struct Integrity* . 2012; 3: 274-284.

18. Houjou K, Takahashi K, Ando K. Improvement of fatigue limit by shot peening for high-tensile strength steel containing a crack in the stress concentration zone. *Int J Struct Integrity* . 2013; 4: 258-266.

19. Yasuda J, Takahashi K, Okada H. Improvement of Fatigue Limit by Shot Peening for High-Strength Steel Containing a Crack like Surface Defect -Influence of Stress Ratio-. *Int J Struct Integrity* . 2014; 5: 45-59.

20. Takahashi K, Osedo H, Suzuki T, Fukuda S. Fatigue strength improvement of an aluminum alloy with a crack-like surface defect using shot peening and cavitation peening. *Eng Fract Mech* . 2018; 193: 151-161.

21. API Recommended Practice 579, Fitness for service, *API Publishing Service (American Petroleum Institute)* , first edition, Washington D.C., Jan. 2000; C3.

22. Yasukawa S, Ohya S, Tango K, Takeda K, Tange A. Microscopic Residual Stress Distribution Measurement on the Surface of Shot Peening. *J Soc Mater Sci (Jap)* . 2014; 63: 655-661.